2009 IEEE International Conference on Robotics and Automation
Kobe International Conference Center
Kobe, Japan, May 12-17, 2009

Aerodynamics of Dragonfly Flight and Robotic Design

Zheng Hu, Raymond McCauley, Steve Schaeffer, and Xinyan Deng

***Abstract*—A pair of dynamically scaled robotic dragonfly model wings was developed to investigate the aerodynamic effect of wing-wing interaction in dragonfly flight. Instantaneous aerodynamic forces were measured while forewing-hindwing phase difference (γ) was systematically varied. Experimental results showed that, i) for hovering flight, γ=0° enhanced the lift force on both forewing and hindwing; γ=180° reduced the total lift force, but was beneficial for vibration suppression and body posture stabilization. In nature, 0° is employed by dragonflies in acceleration mode while 180° is usually in hovering mode. ii) For forward flight, wing-wing interaction enhances forewing lift while reduced hindwing lift at all phase differences. Furthermore, the total lift was slightly reduced for γ=0° to 90° and significantly reduced by 18% when γ=270°. The results consist well with the fact that, dragonflies usually employ 50° to 100° for forward flight, but seldom employ 270°. PIV results are shown for wing-wing interaction analysis.**

I. INTRODUCTION

Dragonflies are one of the most agile and maneuverable flying insect species. They survived millions of year's evolution and are one of the very few species which can intercept preys in air. They can hover, cruise up to 54 km/h, turn 180° in three wing beats, fly sideways, glide, and even fly backwards [1-3]. They intercept prey in the air with amazing speed and accuracy. Their thorax are equipped with wing muscles which accounts for 24% (*Aeshna*) of their body weights, compared to 13% of those of the honey bees [2]. Most dragonflies change their wing motion kinematics for different flight modes such as hovering, cruising and turning. Among these kinematic parameters, the most observed and interesting one is the phase difference (γ) between forewing and hindwing. By definition, it is the phase angle by which the hindwing leads the forewing. When hovering, dragonflies employ 180° phase difference (anti-phase) [1, 4, 5]. When flying forward, they employ phase difference angles from 54° to 100° [6, 7]. When accelerating or performing aggressive maneuvers, they use 0° (in-phase) phase difference [1, 5, 8]. Of various phase angle differences, 270° is rarely observed in dragonfly flight.

There have been a few studies from computational fluid simulations on dragonfly flight [14, 15] and experimental investigations using a pair of vertically stacked robotic wings mimicking flapping flight with horizontal stroke planes [11]. In this study, we investigated two aspects typical of dragonfly flight: the high stroke plane and drag based lift generation. We employ a novel robotic wing apparatus which allows for arbitrary stroke plane angles. The results will contribute to the design of micro aerial vehicles with two pairs of wings.

The authors are with Mechanical Engineering Department, University of Delaware, Newark, DE 19716 USA (e-mail: Deng@udel.edu).This work was supported by the National Science Foundation Award #0545931.

II. EXPERIMENTAL APPARATUS

A. Robotic Dragonfly Model Wings

We constructed a pair of dynamically-scaled robotic model wings (flappers) submerged in a tank of mineral oils and measure the instantaneous aerodynamic forces while replicating dragonfly wing kinematics (Fig. 1).

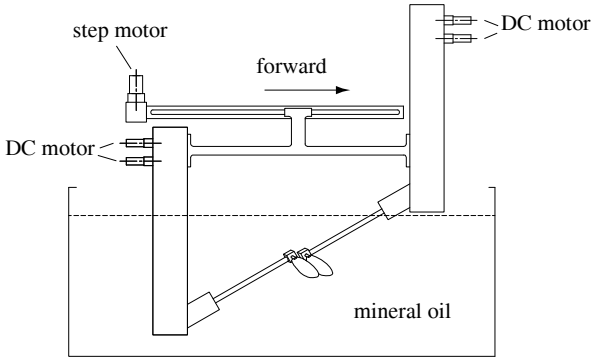

Fig. 1. Sketch of experimental setup.

For each flapper, a bevel-geared robotic wrist was designed to generate motions of three rotational degrees of freedom (stroke, rotation and deviation). The bevel gears transmit the motion from coaxially driven shafts to the wing (Fig. 2). The two wings were placed at close proximity as in dragonflies. The observed deviation angle in dragonfly flight is negligible so that we did not apply deviation to the apparatus. Both wings are mounted on a linear stage driven by a step motor to realize a forward motion.

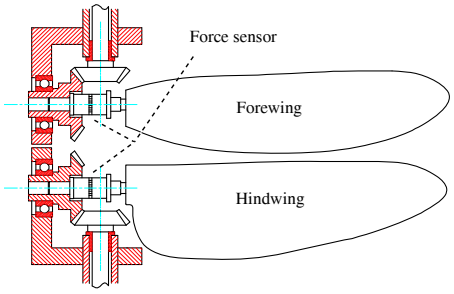

Fig.2. Sketch of wing wrist design

The drive shafts were powered by 16 mm, 0.3 Nm torque DC brush motors (Maxon, Sachseln, Switzerland) equipped with gear heads to reduce speed and magnetic encoders to provide kinematic feedback to ensure motion fidelity. The

motors were driven along kinematic patterns provided by a custom MATLAB (Mathworks, Natick, MA) Simulink program with WinCon software (Quanser Consulting, Ontario, Canada). This software provided commands to the real-time control and data acquisition board (Quanser Consulting, Ontario, Canada) communicating with the hardware. We used Proportional-Integral-Derivative (PID) controllers to run the motors with a precision of 0.1°. Motion commands from the computer were amplified by analog amplifier units (Advanced Motion Control) which directly controlled the input current received by the motor.

Wings were made from Mylar plastic film with a thickness of 0.25 mm which behaves as a rigid wing in our experiments. A carbon fiber rod was glued on the plastic film to serve as the leading edge. The end of the carbon fiber rod was affixed on to the force sensor. The wings have identical geometry as the dragonfly wings but are four times larger with a length of 19 cm for the forewing and 18.5 cm for the hindwing.

The wings along with part of the device were immersed into a tank (46cm × 41cm × 152cm) filled with mineral oil (Kinematic viscosity= 3.4 cSt at 20 °C, density=830 kg/ m^3). This overall set-up enabled us to run the wings along a pre-determined dragonfly kinematics while simultaneously measuring the forces on the forewing and the hindwing respectively (Fig. 1).

B. *Kinematics*

High-speed photos of the dragonfly (*Aeshna juncea*) in hovering flight were taken by Norberg [4]. The body is held almost horizontal, and the wing stroke plane is tilted 60° (β) relative to the horizontal line. For both forewing and hindwing, the chord is almost horizontal during the downstroke and is close to being vertical during the upstroke (Fig.3); the stroke frequency (n) is 36 Hz, the stroke amplitude (Φ) is 60°; the stroke angle (ϕ_f) is from 35° above the horizontal to 25° below for forewing, and (ϕ_h) is from 45° above to15° below for hindwing; the hindwing leads the forewing in phase by 180°. The mass of the insect (m) is 754mg; forewing length (r_f) is 4.74 cm; hindwing length (r_h) is 4.60 cm; the mean chord lengths of the forewing and hindwing are 0.81 cm and 1.12 cm, respectively.

Azuma [10] filmed a slow climbing flight of a dragonfly (*Sympetrum Frequens*) with a high speed camera (873 frames per second). He showed that the flapping trajectory can be well represented by a sinusoidal function, as shown in Fig.4.

Based on morphology and kinematics data, the reference velocity of the dragonfly wing is $U = 2\Phi n r_2 = 2.1\text{ms}^{-1}$, and the Reynolds number is $Re = Uc/\upsilon \approx 1160$. The advance ratios considered in forward study is J=0.35, corresponding to forward flight speed (V) of 1.3 m/s.

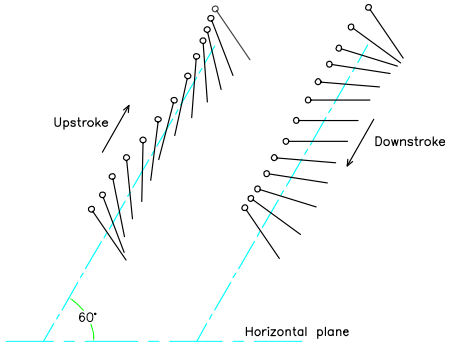

Fig. 3. Sketches of the dragonfly wing kinematics during upstroke and downstroke. Solid lines denote the wing chord section; circles denote the leading edge. Both forewing and hindwing apply.

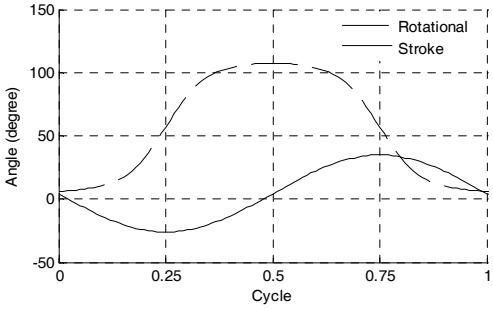

Fig. 4. Forewing flapping trajectory: stroke angle (solid) and rotational angle (dash). Hindwing trajectory is the same except a 10° stroke angle offset.

C. *Force Measurement*

The forces as well as torques on the moving wings can be measured by a six-component force sensor (ATI NANO-17, Apex, NC), with a range of ±12 N for force and ±0.5 Nm for torque along three orthogonal axes. The amplitude of forces in this study falls in a range of ±1N. Errors for each measurement do not exceed 0.005N. Using appropriate trigonometric conversions, these force measurements were then converted to lift and thrust forces in the earth coordinates. Note that in this study, lift is defined as the vertical component of the aerodynamics force and thrust the horizontal component in global coordinate frame.

The force measured from the sensor is a combination of wing aerodynamic force, wing gravity (plus buoyancy in oil) and wing inertial force. To extract the aerodynamic information from the raw data, we first subtract the gravity (plus buoyancy in oil) of wing. This can be done directly by measuring the static forces of wing in oil. We estimated the contribution of wing inertial forces analytically, assuming that all mass of the wing (m_w=1.5 g) is concentrated at the wing center of mass. The inertia force along the stroke plane direction caused by stroke angular acceleration is calculated similar to [11]:

$$F_x^*(t) = m_w l_x \ddot{\phi} \tag{1}$$

in which l_x (11.3cm) is the first moment arm, t is time, $\ddot{\phi}$ is the stroke angular acceleration. After calculation we found the magnitude of the wing inertia force is 1.7 mN, which counts

for less than 1% of the total force measured by the sensor. Thus, the inertial force components can be neglected.

D. Force Scaling and Force Coefficient Calculation

The aerodynamic forces acting on an actual dragonfly, F_{fly}, is related to those measured in the robotic model, F_{robot}, according to the following scaling rule [12]:

$$F_{fly} = F_{robot} \cdot \frac{\rho_{air}}{\rho_{oil}} \cdot \left(\frac{n_{fly}}{n_{robot}}\right)^2 \cdot \left(\frac{r_{fly}}{r_{robot}}\right)^2 \cdot \frac{S_{fly}}{S_{robot}} \cdot \frac{\hat{r}_{2fly}^2}{\hat{r}_{2robot}^2} \quad (2)$$

where ρ is fluid density, n is stroke frequency, r is wing length, S is wing area, and $\hat{r}_2$ is the normalized second moment of wing area.

In this study, total lift and thrust force coefficient are defined similar to[13] [14]:

$$C_l = L/[0.5\rho U^2(S_f + S_h)(1 + J\cos\beta)^2] \quad (3)$$

$$C_t = T/[0.5\rho U^2(S_f + S_h)(1 + J\cos\beta)^2] \quad (4)$$

L and T denote the lift and thrust forces. The reference velocity is calculated to be $U = 2\Phi n r_2 = 2.1\text{ms}^{-1}$; S_f and S_h are the areas of forewing and hindwing, respectively. Advance ratio (J) is 0 in the hovering case.

Accordingly, we define lift and thrust coefficient for a single wing. For example, for forewing:

$$C_{l,f} = L_f/[(0.5\rho U^2 S_f)(1 + J\cos\beta)^2] \quad (5)$$

$$C_{t,f} = T_f/[(0.5\rho U^2 S_f)(1 + J\cos\beta)^2] \quad (6)$$

III. Results and Discussion

A. Forces scaled to the real dragonfly

We first replay the hovering kinematics of dragonfly when the forewing and hindwing are out-of-phase (180°), which is most commonly observed in dragonfly hovering. The results show an average lift force of 0.0711 N on the forewing and 0.082 N on the hindwing during one wingbeat cycle. The average thrust forces are 0.001 N on the forewing and 0.003 N on the hindwing.

We then apply (2) to scale the lift force back to those of a true dragonfly. The resulted average lift force is 187 mg on a forewing and 216 mg on a hindwing. The total average lift on a four-winged dragonfly is therefore (187+216)*2=806 (mg). This result is comparable to the 754 mg body mass measured in [9]. On the other hand, the total average thrust force is almost zero when compared with the average lift force, which follows the hovering condition that the thrust should be zero.

B. Effect of Phase Difference in Hovering Flight

We measured the forces with the same kinematics of hovering and systematically vary the phase differences from 0° to 360° in steps of 30°. The resulting average lift and thrust coefficients are plotted in Fig. 5.

Fig. 5 shows the averaged force coefficients in hover. As the phase difference tends to 0°, forces tend to be higher, and reach their maximum on 0°. The forces get lower values when γ is around 180°. As shown in Fig. 5, in range 330° to 30°, the wing-wing interaction enhances the total lift force by up to 6%; in range 150° to 180°, interaction decreases the total lift force by up to 9%. This provides direct evidence that in-phase flight generates larger aerodynamic forces than anti-phase flight, and also larger than the case without wing-wing interaction. This may explain the behavior that dragonfly flies in-phase in case of accelerating or maneuverings that calls for a high force generation.

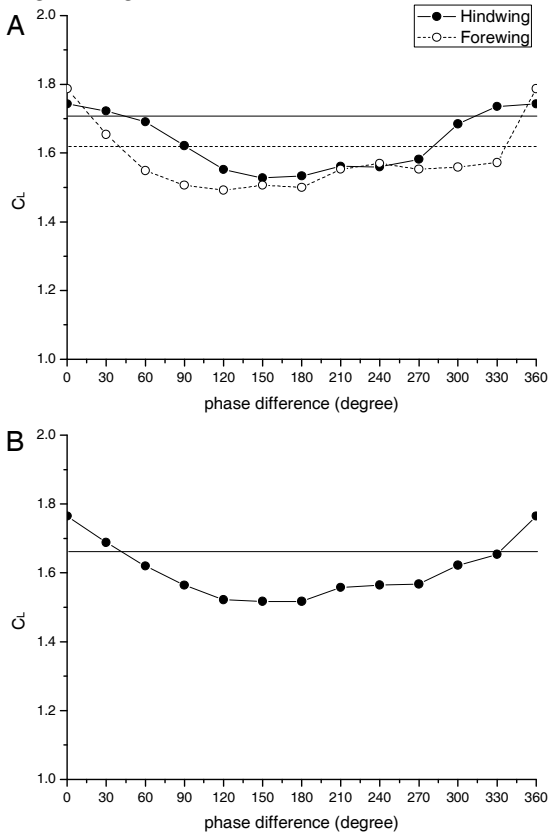

Fig. 5. Force coefficients results for hovering flight test. A) Lift coefficients on forewing and hindwing respectively; B) Total lift coefficients on both wings. The straight lines in each plot indicate the force results without interaction.

Fig. 6 shows a PIV result for anti-phase hovering. Based on the interaction flow pattern, we may be able to explain the effects of phase differences. With 180° phase difference, hindwing is at its midway of downstroke when forewing is at its midway of upstroke, which corresponds to Fig. 6. At this moment, the surrounding area of hindwing is occupied by a large scale of downwash, a part of which comes from the previous stoke of forewing. We call this a kind of interaction flow. Thus, hindwing is flapping in a downwash environment during its downstroke so that it is subjected to an aerodynamic pressure loss. This could be a reason for the hindwing lift loss in 180° case compared to single hindwing case, and the loss mainly happens around the midway downstroke.

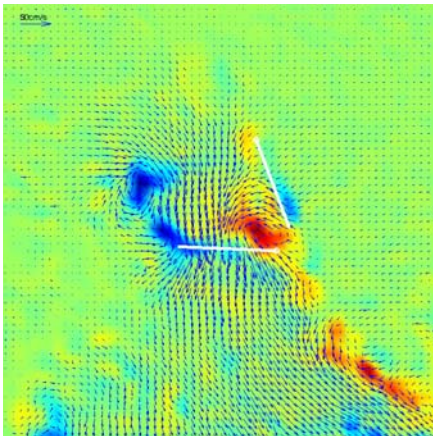

Fig. 6. Particle image Velocimetry (PIV) result for $\gamma = 180°$ in hovering. The wing on the right side is forewing; the other is hindwing.

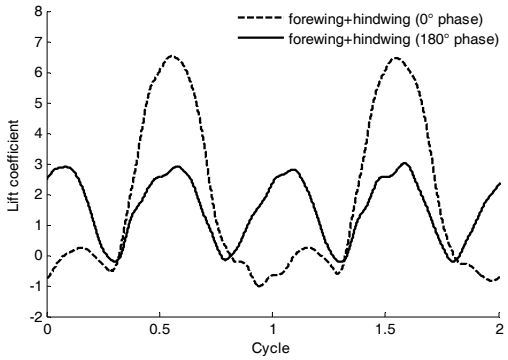

Fig. 7. Comparison between total lift forces generated when hovering with $\gamma = 0°$ and $\gamma = 180°$ respectively.

In order to find out the possible reason that dragonfly uses anti-phase style for hovering mode, we need to compare the time traces of total lift forces generated by $\gamma = 0°$ with those generated by $\gamma = 180°$ (Fig.7). It was noted that anti-phase produces uniform flight, whereas flight produced by in-phase stroking is irregular [5]. Fig.7 shows the instantaneous lift force coefficients comparison between in-phase and anti-phase flight. As we can see, in-phase brings larger irregularity in the aerodynamic forces than anti-phase does. Observing from the time trace curve for in-phase hovering, there exists a 1/2 cycle period when lift force is closed to zero, while in another 1/2 cycle the peak value is two times of the peak value for anti-phase flight, because forewing and hindwing peak overlap. This irregularity of instantaneous forces increases the body vibration when hovering, while for anti-phase flight the inequality can be compensated to some extent by evenly distributing the peak forces of forewing and hindwing on the whole cycle. Besides minimizing the force irregularities and keeping body posture stable, anti-phase flight can also save energy that might be lost in body vibration [15]. It was shown that wing-wing interaction save aerodynamic power during anti-phase hovering [15, 16]. Thus, it is reasonable that dragonflies would rather lose 15% force production for improving flight stability and vibration suppression as well as power efficiency.

C. *Effect of Phase Difference in Forward Flight*

The average lift coefficients and average thrust coefficients in forward flight are plotted in Fig. 8. During forward flight, wing-wing interaction always enhances the forewing lift while reducing hindwing lift generation no matter how much γ is. Lift on forewing is enhanced by at most 23% when flapping in-phase and at least 4% when phase difference falls into 120°~330°; On the other hand, lift on hindwing reaches maximum on 60° and minimum on 270°. Hindwing is subjected to a severe loss on force production up to 38% around 270°. The total force is also minimized around 270°.

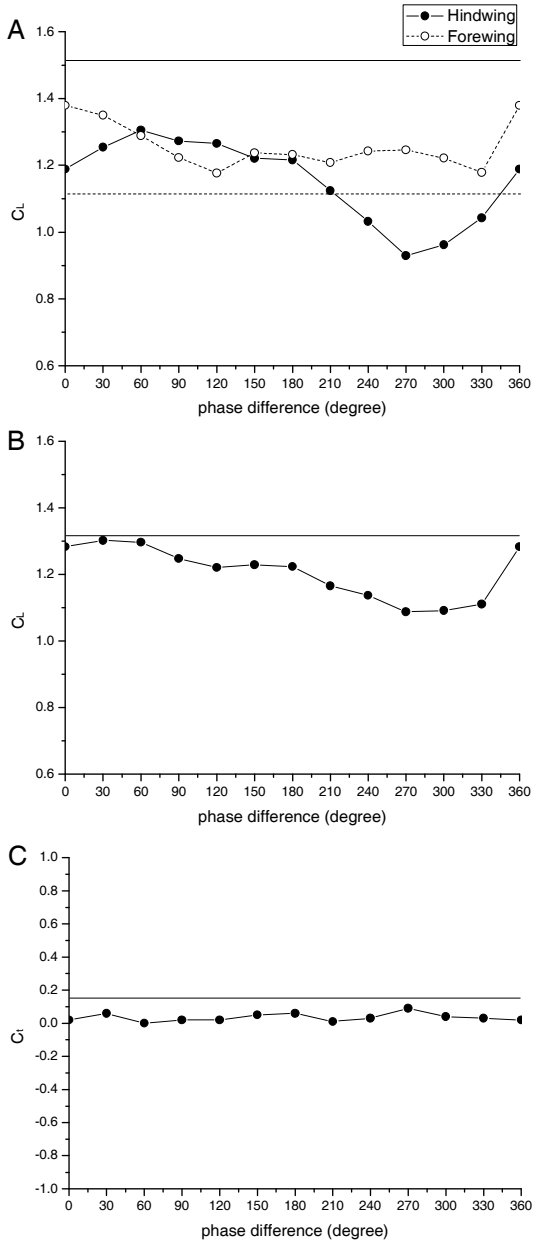

Fig. 8. Force coefficients results for forward flight test. A) Lift coefficients on forewing and hindwing respectively; B) total average lift coefficients on both wings; C) total average thrust coefficients on both wings. The straight lines in each plot indicate the force results without interaction.

We can also distinguish the case $\gamma = 90°$ and the case $\gamma = 270°$: the former one can offer dragonfly an 18% higher force than the latter one. On the other hand, 270° offers similar vibration and stability properties as 90°. This may explain why dragonfly never favors the 270° phase difference.

The above results agree qualitatively with the CFD results from [14] and [17] to some extent. Their conclusion is that the forewing is only slightly influenced by the wing–wing interaction, but the hindwing lift is greatly reduced by 20~60% during forward flight with a 180°~360° phase difference, compared with that of a single hindwing. Our results show that there are obvious lift enhancements on the forewing.

Fig.9 compares the time traces of hindwing lift among the cases of single hindwing, γ=90° and $\gamma = 270°$. We note that the lift in case of γ=270° was considerably reduced when compared with other cases, and the reduction mainly occurred when hindwing was in the midway of downstroke. This is reasonable because a large portion of lift is produce during this period, since wings reach the highest flapping speed and largest angle of attack around the midway of downstroke.

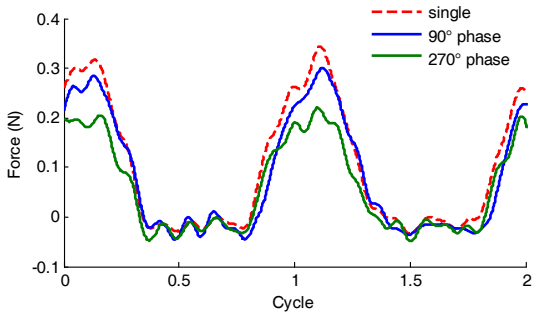

Fig. 9. Comparisons of instantaneous hindwing lift in forward flight among the cases of single hindwing, γ = 90° and γ = 270°.

Fig. 10 shows the PIV result of $\gamma = 270°$ in forward flight. At this instance, the forewing is at the end of downstroke while the hindwing is around midway of downstroke. Again we notice the hindwing is confronted with the downward interaction flow from the forewing. This explains the force reduction on hindwing at 270°. Compared with the interaction mechanism of hovering case, a main difference is that the confronting time is about a quarter cycle ahead in forward flight, because hindwing enters into the downwash area positively since it has a forward speed.

For thrust force measurement, a systematic series of wind-tunnel tests on an ornithopter configuration consisting of two sets of symmetrically flapping wings, located one behind the other in tandem, was previously performed [18]. It was found that the tandem arrangement can increase thrust for certain phase differences and longitudinal spacing between the wing sets. In particular, close spacing on the order of one chord length is generally best, and phase differences of approximately -50° to 50° give the highest thrusts and propulsive efficiencies. Nevertheless, this conclusion does not apply for the dragonfly flight. Instead, the thrust plot above indicates a drop on thrust force caused by interaction, no matter what the phase difference is. The difference is due to the difference in wing kinematics as well as the fact that the space between forewing and hindwing of dragonfly is much smaller that the one chord spacing.

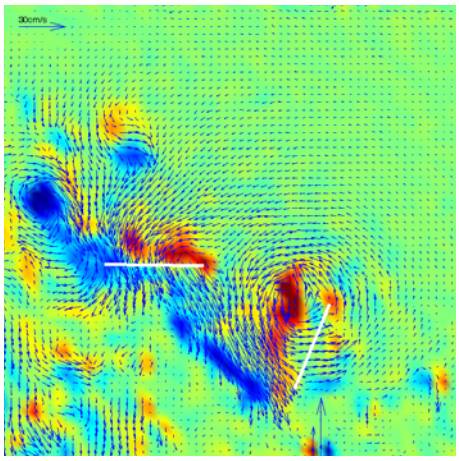

Fig. 10. Particle image Velocimetry (PIV) results for γ = 270° in forward flight. The wing on the right side is forewing; the other is hindwing.

IV. DRAGONFLY-INSPIRED MAV

We have developed several dragonfly robots, and Fig. 11 shows one of our latest designs. This model has two separate pairs of wings driven by a double crank rocker mechanism.

The current prototype weighs 4g including battery and electronics. This prototype was able to generate 28Hz flapping frequency while mounted with four carbon fiber leading edges only, and 9 Hz after attaching (gluing) the polymer wings onto two leading edges. With all four wings attached the frequency reduced to 7Hz. Table 1 shows physical specifications.

In order to test different wing materials, we have developed a mechanical wing tester. It can be used to study the fatigue cycles of each wing developed and can also be used to visualize the wing kinematics by a high speed camera. Fig.12 shows the wing tester and the camera images of wing test.

Fig. 11. Dragonfly M.A.V prototype

Table 1. Dragonfly prototype specifications.

Motor	Battery & Control	Gear
Torque: 44mNm	4V	Maximize Torque
Power: 176mW	0.4A	Ratio: 1:7
16k rpm	Infrared Chip	Precision Molded
Weight: 1.4g	Weight:1.1+1.3g	Weight:0.23g

Fig 12. Wing tester and camera images of a test wing at 20Hz.

The average size of the wings is bigger compared to real insects under our investigation. Veins are added for added rigidity to generate higher force. With reduced length and size, the frequency becomes higher. This process requires much trial and error as small variations in wing structure can cause it to tear apart at high frequencies. Dragonflies have a lot of characteristics naturally build into their wings. Further tests will be aimed to finding out what makes their wings so robust yet so delicate under high frequencies.

V. Conclusion

The experiments described here investigate the effect of forewing-hindwing interactions during hovering and forward flight of dragonfly. Overall, wing-wing interaction reduces the total lift force generation. In hovering, dragonflies use anti-phase flight which generates a regular lift force for stability and vibration reduction purposes. In forward flight, lift force is enhances in forewing while reduced in hindwing due to the downwash from forewing. In-phase flight generates higher lift than other phase differences, while 270° phase difference generates the lowest lift. PIV results provide some analysis for wing-wing interaction mechanism. A prototype for dragonfly-inspired M.A.V has been shown. On-going and future work involves the development of dragonfly robots with high flapping frequencies.

References

[1] D. E. Alexander, "Unusual phase relationships between the forewings and hindwings in flying dragonflies," *J Exp Biol*, vol. 109, pp. 379-383, 1984.

[2] F. M. Appleton, "Dragonflies and flight," *Nature Canada*, vol. 3(3), pp. 25-29, 1974.

[3] F. C. Whitehouse, " British Columbia dragonflies (Odonata), with notes on distribution and habits," *The American Midland Naturalist*, vol. 26(3), pp. 488, 1941.

[4] R. A. Norberg, "Hovering flight of the dragonfly: Aeschna juncea L., kinematics and aerodynamics," *Swimming and Flying in Nature*, vol. 2, pp. 763-780, 1975.

[5] G. Rüppell, "Kinematic analysis of symmetrical flight manoeuvres of odonata," *J Exp Biol*, vol. 144, pp. 13-42, 1989.

[6] A. Azuma and T. Watanabe, "Flight performance of a dragonfly," *J Exp Biol*, vol. 137, pp. 221-252, 1988.

[7] H. Wang, L. Zeng, H. Liu, and C. Yin, "Measuring wing kinematics, flight trajectory and body attitude during forward flight and turning maneuvers in dragonflies," *J Exp Biol*, vol. 206, pp. 745-57, 2003.

[8] A. L. Thomas, G. K. Taylor, R. B. Srygley, R. L. Nudds, and R. J. Bomphrey, "Dragonfly flight: free-flight and tethered flow visualizations reveal a diverse array of unsteady lift-generating mechanisms, controlled primarily via angle of attack," *J Exp Biol*, vol. 207, pp. 4299-323, 2004.

[9] R. A. Norberg, "The pterostigma of insect wings and inertial regulator of wing pitch," *J. Comp. Physiol*, vol. 81, pp. 9-22, 1972.

[10] A. Azuma, S. Azuma, I. Watanabe, and T. Furuta, "Flight mechanics of a dragonfly," *J Exp Biol*, vol. 116, pp. 79-107, 1985.

[11] W. J. Maybury and F. O. Lehmann, "The fluid dynamics of flight control by kinematic phase lag variation between two robotic insect wings," *J Exp Biol*, vol. 207, pp. 4707-26, 2004.

[12] S. N. Fry, R. Sayaman, and M. H. Dickinson, "The aerodynamics of hovering flight in Drosophila," *J Exp Biol*, vol. 208, pp. 2303-18, 2005.

[13] W. B. Dickson and M. H. Dickinson, "The effect of advance ratio on the aerodynamics of revolving wings," *Journal of Experimental Biology*, vol. 207, pp. 4269-4281, 2004.

[14] J. K. Wang and M. Sun, "A computational study of the aerodynamics and forewing-hindwing interaction of a model dragonfly in forward flight," *J Exp Biol*, vol. 208, pp. 3785-804, 2005.

[15] Z. J. Wang and D. Russell, "Effect of forewing and hindwing interactions on aerodynamic forces and power in hovering dragonfly flight," *Physical Review Letters*, vol. 99, pp. -, 2007.

[16] J. R. Usherwood and F. O. Lehmann, "Phasing of dragonfly wings can improve aerodynamic efficiency by removing swirl," *J R Soc Interface*, 2008.

[17] H. Huang and M. Sun, "Dragonfly forewing-hindwing interaction at various flight speeds and wing phasing," *AIAA J.*, vol. 45, pp. 508-511, 2007.

[18] J. Warkentin and J. DeLaurier, "Experimental aerodynamic study of tandem flapping membrane wings," *AIAA J.*, vol. 44, pp. 1653-1661, 2007.